

Current-induced macrospin *vs.* spin-wave excitations in spin valves

Arne Brataas,¹ Yaroslav Tserkovnyak,² and Gerrit E. W. Bauer³

¹*Department of Physics, Norwegian University of Science and Technology, N-7491 Trondheim, Norway*

²*Lyman Laboratory of Physics, Harvard University, Cambridge, Massachusetts 02138, USA*

³*Kavli Institute of NanoScience, Delft University of Technology, Lorentzweg 1, 2628 CJ Delft, The Netherlands*

(Dated: December 2, 2024)

The mode dependence of current-induced magnetic excitations in spin valves is studied theoretically. The torque exerted on the magnetization by transverse spin currents as well as the Gilbert damping constant are found to depend strongly on the wave length of the excitation (spin wave). Analytic expressions are presented for the critical currents that excite a selected spin wave. The onset of macrospin (zero wavelength) *vs.* finite wavelength instabilities depends on the device parameters and the current direction, in agreement with recent experimental findings.

PACS numbers: 75.70.Cn, 72.25Mk

Less than a decade ago Berger [1] and Slonczewski [2] argued that an electric current sent through multilayers of normal metals (N) and ferromagnets (F) can excite the ferromagnetic order parameter and even reverse the magnetization. The theoretical predictions have been confirmed by many experiments on F|N|F nanostructured spin valves [3, 4]. The physics of collective ferromagnetic excitations driven by out-of-equilibrium quasi-particles is complex and fascinating. In magnetic memories current-induced magnetization switching might turn out to be superior to its magnetic field driven counterpart.

Current-induced magnetic excitations are driven by the spin torque acting on the magnetic order parameter when a spin current polarized normal to the magnetization is absorbed by the ferromagnet [1, 2, 5, 6]. The transverse spin current extinction is a quantum mechanical interference effect between electrons at the Fermi energy with different precession lengths. In Co, Ni and Fe this happens on an atomistic length scale [5, 6]. By conservation of angular momentum the absorbed spin current acts as a torque on the ferromagnetic condensate. At a critical spin current, this torque becomes strong enough to set the magnetization into motion, possibly leading to a complete reversal of the magnetization direction.

Starting from the prediction of the current-induced magnetization dynamics an unsettled discussion rages. Whereas Berger considers an onset of spin wave excitations as the main cause of a finite critical current, Slonczewski considers a rigid coherent rotation of the whole magnet (“macrospin” model) that starts at a critical current corresponding to a torque that just overcomes the Gilbert damping. In our view, the differences in these pictures are to some extent semantic, since the macrospin model is identical to the lowest energy spin wave. The physical question addressed here is the wavelength of the spin wave that is most easily excited. We find that there is no universal answer and that the preferential excitation mode depends on device parameters and current direction. Nevertheless, our theory agrees well with experiments that observe both type of excitations [12].

Most theories of spin torques and critical currents are based on macrospin precessions in spin valves [2, 6]. Indeed, sufficiently small magnetic clusters support a single domain magnetization and the magnetic field induced magnetization reversal is well described by a coherent rotation according to the Stoner-Wohlfarth model [7]. From a theoretical point of view, the macrospin models validity is essential for understanding the non-linear physics underlying the entire magnetization dynamics by dynamical systems theory and the probabilistic treatment in the “presence” of noise [9]. In a single ferromagnetic film sandwiched by normal layers the torque on the macrospin domain necessarily vanishes. However, biased N|F|N structures are unstable with respect to spin waves with shorter wavelengths [10, 11]. In spin valves, we may therefore expect a competition between macrospin and shorter wave length spin waves excitations. Experiments on spin valves [12] have indeed been interpreted in terms of both types of excitations, depending on the current direction. It is our purpose to understand and model these data in order to assess the dependence of the excitation modes on device parameters. Another motivation to study the competition between different excitation modes is the need to find criteria for the breakdown of simple models for the magnetization that provide a guide for the necessity of full-fledged micromagnetic calculations [13].

Our work extends Refs. [10, 11] on single layers to spin valves. We derive analytical expressions for bias-driven spin torques, enhanced Gilbert damping constants [8] and critical currents for magnetic excitations as a function of wave vector. We predict a rich “phase diagram” in the current *vs.* magnetic field plane.

We consider N|F|N|F|N spin-valve pillars in Fig. 1 in the semiclassical transport regime where magneto-electronic circuit theory applies [5]. Our disregard of spin flip in F is allowed for sufficiently thin F films and considerably simplifies the calculations. We also consider normal metals thinner than the spin-diffusion length. We solve the diffusion equations in the bulk of each material *and* include the resistances due to the interfaces be-

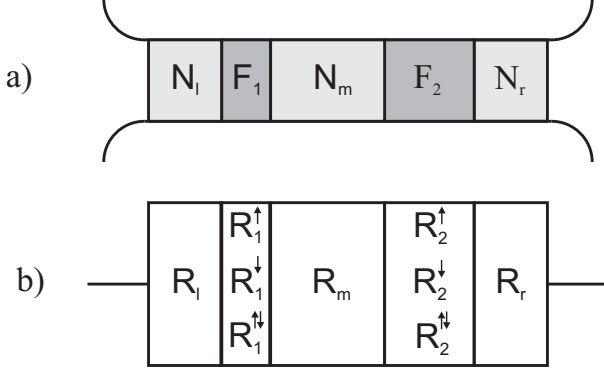


FIG. 1: a) Spin-valve with b) circuit resistance elements.

tween the materials. The spin-dependent resistances R_i^s ($i = 1, 2, s = \uparrow, \downarrow$) in the ferromagnetic elements consist of interface and bulk contributions: $R_i^s = 2R_{F_i/N}^s + \varrho_{F_i}^s t_{F_i}$, where $R_{F_i/N}^s$ is the spin-dependent resistance per unit area of a single F|N interface assumed identical on both sides of film i . $\varrho_{F_i}^s$ and t_{F_i} are its spin-dependent resistivity and thickness. We also find it convenient to introduce a mixing resistance $R_i^{\uparrow\downarrow} = 1/(2G_i^{\uparrow\downarrow})$. The mixing conductance $G_i^{\uparrow\downarrow}$ governs the transport of spins transverse to the magnetization direction and determines the spin torque [5]. Similarly, the resistances in the normal metal elements are R_l , R_m and R_r , respectively.

We start from a collinear parallel or antiparallel spin valve configuration. We consider small transverse instabilities of the magnetization in Fourier space, $\delta\mathbf{m}_1^{\perp}(\mathbf{q})$ and $\delta\mathbf{m}_2^{\perp}(\mathbf{q})$. In order to manage the analytical spin torque expressions obtained by tedious algebra, we introduce the following standard notation for the i th ferromagnet: average resistance $R_i^* = (R_i^{\uparrow} + R_i^{\downarrow})/4$ and polarization $P_i = (R_i^{\downarrow} - R_i^{\uparrow})/(R_i^{\uparrow} + R_i^{\downarrow})$. The resistance contrast between parallel ($P_1 P_2 > 0$) and antiparallel ($P_1 P_2 < 0$) configurations is $\Delta R = R^{\text{ap}} - R^{\text{p}} = (4R_1^* R_2^* |P_1 P_2|)/(R_l + R_1^* + R_m + R_2^* + R_r)$. The polarization of the current is $P_t = (R_1^* P_1 + R_2^* P_2)/(R_l + R_1^* + R_m + R_2^* + R_r)$. The charge current is denoted $j^{(c)}$.

The spin torque on ferromagnet i has contributions from electrons hitting it from the left and the right, $\tau_i = \tau_{il} + \tau_{ir}$. $\tau_{1l} = \mathcal{L}_{1l} \delta\mathbf{m}_1^{\perp} j^{(c)}$ on the first ferromagnet exerted by electrons coming from the left and $\tau_{2r} = \mathcal{L}_{2r} \delta\mathbf{m}_2^{\perp} j^{(c)}$ on the second ferromagnet due to electrons from the right is given by:

$$\mathcal{L}_{1l} = \frac{R_l [f_l(0) - f_l(q)]}{R_l f_l(q) + R_1^{\uparrow\downarrow}} \frac{R_1^* P_1 + R_2^* P_2}{R_l + R_1^* + R_m + R_2^* + R_r}. \quad (1)$$

Expression for \mathcal{L}_{2r} are obtained by changing sign and substituting l by r and 1 by 2. Here $f(x) = \tanh(x)/x$, $f_l(q) = f[x_l(q)]$, and $x_l(q) = (q^2 + l_l^{-2})^{1/2} t_{Nl}$, where t_{Nl} is the left normal metal thickness and l_l its spin-diffusion length. In particular $f_l(0) \approx 1$ (and similarly for f_m , f_r , and x_m , x_r). For a single ferro-

magnetic layer these torques vanish in the long wavelength limit as in Ref. [10]. The new physics is contained in the wave vector-dependent torques τ_{1r} and τ_{2l} . In the expressions $\tau_{1r} = (\mathcal{L}_{1r} \delta\mathbf{m}_1^{\perp} + \mathcal{K}_{1r} \delta\mathbf{m}_2^{\perp}) j^{(c)}$ and $\tau_{2l} = (\mathcal{L}_{2l} \delta\mathbf{m}_2^{\perp} + \mathcal{K}_{2l} \delta\mathbf{m}_1^{\perp}) j^{(c)}$, the spin torques due to spin currents between the two ferromagnets are found as:

$$\mathcal{L}_{1r} = \frac{-(n_1 + n_2 x_m^2 + n_3/f_m) / R^*}{R_m^2 + R_1^{\uparrow\downarrow} R_2^{\uparrow\downarrow} x_m^2 + R_m (R_1^{\uparrow\downarrow} + R_2^{\uparrow\downarrow}) / f_m}. \quad (2)$$

where, $n_1 = -R_m^2 (P_1 R_1^* + P_2 R_2^*)$, $n_2 = R_2^{\uparrow\downarrow} [P_1 R_1^* (R_2^* + R_m + R_r) - P_2 R_2^* (R_l + R_1^*)]$, $n_3 = n_1 R_2^{\uparrow\downarrow} / R_m + n_2 R_m / R_2^{\uparrow\downarrow}$ introducing $R^* = R_l + R_1^* + R_m + R_2^* + R_r$. The expressions for \mathcal{L}_{2l} is similar to that for \mathcal{L}_{1r} , with an overall sign change and the substitution $l \leftrightarrow r$ and $1 \leftrightarrow 2$. \mathcal{K}_{1r} and \mathcal{K}_{2l} govern the dynamic coupling between the ferromagnets, but do not affect the instabilities of individual ferromagnets and are therefore not discussed here. In the limit of long-wavelength excitations, $q \rightarrow 0$, our results reduce to previous ones [5, 14].

Let us discuss the spin torques (1) and (2) in simple limits. For *symmetric* junctions in a parallel magnetic configuration $R_l = R_r$, $R_1^{\uparrow\downarrow} = R_2^{\uparrow\downarrow}$, $R_1^* = R_2^*$, and $P_1 = P_2$. For macrospin ($q = 0$) excitations $\mathcal{L}_{1l} = 0$ and $\mathcal{L}_{1r} = P_t/2$, illustrating that the spin torque is exerted by electrons coming from ferromagnet 2 that hit ferromagnet 1 from the right and is governed by the polarization of the entire spin-coherent region P_t [14]. At short wavelengths, $\mathcal{L}_{1r} = -(P_t/2) R_m / R_1^{\uparrow\downarrow}$ and $\mathcal{L}_{1l} = (P_t/2) R_l / R_1^{\uparrow\downarrow}$, so that $\mathcal{L}_1 = \mathcal{L}_{1l} + \mathcal{L}_{1r} = -(P_t/2) (R_m - R_l) / R_1^{\uparrow\downarrow}$. It is the asymmetry in the diffusion process to the left and to the right of the ferromagnet that determines the sign of the short wavelength spin torque [10]. When $R_m = R_l$, small wavelength modes cannot be excited. In the limit $R_l = 0$ there is no short wavelength spin torque from electrons that hit ferromagnet 1 from the left and vice versa when $R_m = 0$ we find $\tau_{1r}(q \rightarrow 0) \rightarrow 0$. On the other hand, the macrospin, torque in symmetric junctions only depends on the global polarization for symmetric junctions [14]. We thus provided proof of the conjecture in Ref. [12] that the spin torque \mathcal{L}_{1r} can change its sign as a function of q when $R_m > R_l$ for symmetric junctions. In that case, the magnetization moves as a macrospin for one current direction but short wavelength spin waves are excited when the current is reversed. In general, we find that when the normal-metal bulk resistance asymmetry is smaller than the interface spin-mixing resistance the macrospin spin torque is larger than the short wavelength spin torque. For strongly asymmetric structures, \mathcal{L}_{1r} is negative also for long-wavelength excitations [14].

The critical current for the onset of magnetic instabilities depends also on spin-pumping by a moving magnetization that opposes the dynamics [8]. Spin pumping by ferromagnet i into neighboring normal metals $\propto G_i^{\uparrow\downarrow} \mathbf{m}_i \times \frac{\partial \mathbf{m}_i}{\partial t}$ enhances the Gilbert damping $\alpha_i =$

$\alpha_i^{(0)} + \alpha'_{il} + \alpha'_{ir}$, where $\alpha_i^{(0)}$ is the damping parameter in the isolated ferromagnet. Spin pumping to the left gives [10] $\alpha'_{il} = \eta_1 R_K / [R_1^{\uparrow\downarrow} + R_l f_l(q)]$, where $\eta_1 = \gamma^* / (8\pi M_1 V_1)$, γ^* is the gyromagnetic ratio, M_i and V_i are the magnetization and volume of ferromagnet i , and $R_K = h/e^2$ is a conductance quantum. The enhancement due to spin pumping into the middle normal metal comprises a new result:

$$\alpha'_{1r} = \frac{\eta_1 R_K \left(R_2^{\uparrow\downarrow} x_m^2 + R_m / f_m \right)}{R_m^2 + R_1^{\uparrow\downarrow} R_2^{\uparrow\downarrow} x_m^2 + R_m \left(R_1^{\uparrow\downarrow} + R_2^{\uparrow\downarrow} \right) / f_m}. \quad (3)$$

Both α'_{il} and α'_{1r} can be understood in terms of an effective resistance against pumping spins out of the ferromagnet. Spin pumping to the left is limited by the wavelength-dependent effective total resistance $R_1^{\uparrow\downarrow} + R_l f_l$. In the long-wavelength limit the resistors are in series, $R_1^{\uparrow\downarrow} + R_l$. In the short-wavelength limit, the effective resistance is reduced due to the inhomogeneous spin distribution. Spin pumping to the right, in the long-wavelength limit governed by $R_1^{\uparrow\downarrow} + R_m + R_2^{\uparrow\downarrow}$ is also reduced in the short-wavelength limit. For the second ferromagnet, we compute $\alpha_2 = \alpha_2^{(0)} + \alpha'_{2l} + \alpha'_{2r}$ with identical expression as above with $1 \leftrightarrow 2$ and $l \leftrightarrow r$.

Including spin torques and enhanced damping, the magnetization dynamics obey a generalized Landau-Lifshitz-Gilbert equation:

$$\frac{\partial \mathbf{m}_i}{\partial t} = -\gamma \mathbf{m}_i \times \mathbf{H}_{\text{eff}} + \frac{\gamma^*}{2eM_i t_{Fi}} \boldsymbol{\tau}_i + \alpha_i \mathbf{m}_i \times \frac{\partial \mathbf{m}_i}{\partial t}. \quad (4)$$

The effective magnetic field \mathbf{H}_{eff} is the functional derivative of the total magnetic energy U due to external magnetic field, magnetic anisotropy and spin-wave stiffness. To lowest order in the excitation amplitude $U = -\mathbf{m}_i^{(0)} \cdot \mathbf{x}H + K_1(\mathbf{u}_1 \cdot \delta \mathbf{m}_i^{\perp})^2 + K_2(\mathbf{u}_2 \cdot \delta \mathbf{m}_i^{\perp})^2$, where the applied magnetic field H is assumed to be along the initial magnetization direction. At $q = 0$, K_1 and K_2 are anisotropy constants along axes \mathbf{u}_1 and \mathbf{u}_2 ; for finite q , they also represent spin-wave stiffness.

A configuration in which ferromagnet 1 is aligned parallel with the external magnetic field becomes unstable when $j^{(c)} > j_1^+$, whereas an antiparallel magnetization becomes unstable when $j^{(c)} < j_1^-$. We compute the critical currents at $T = 0$ requiring that the damping torque is exactly canceled by the spin torque:

$$j_1^{\pm} = \frac{\alpha_1^{(0)} + \alpha'_{il} + \alpha'_{1r}}{\mathcal{L}_{1l}^{\pm} + \mathcal{L}_{1r}^{\pm}} \frac{2e}{\hbar} M_1 t_{F1} \frac{\omega^{\pm}}{\gamma^*}, \quad (5)$$

introducing the ferromagnetic resonance frequencies $\omega^{\pm} = H \pm (K_1 + K_2)/2$. \mathcal{L}_{1L}^{\pm} and \mathcal{L}_{1R}^{\pm} denote spin torques computed for positive/negative polarization, $P_1 = \pm |P_1|$. When the torques change sign as a function of wave vector the ferromagnet can be unstable against macrospin excitations when the current is flowing in one

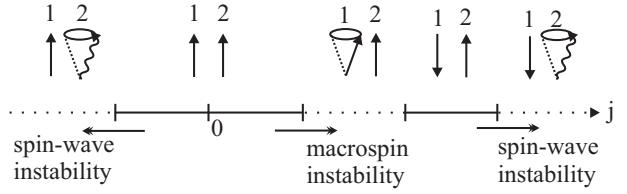


FIG. 2: Phase diagram for ferromagnet 1 and 2, starting in a parallel configuration, as a function of current.

direction, but spin-waves are excited when the current is reversed, as pointed out above. Similar expressions hold for j_2^{\pm} the critical current for ferromagnet 2, j_2^{\pm} .

We are now in position to discuss experiments [12]. A good measure of the efficiency of the spin torques is the critical current $\partial j_i / \partial H$ at high magnetic fields when anisotropies K_1 and K_2 do not play a role [16]. The magnetoresistance, enhanced Gilbert damping, spin torques and switching current all depend strongly on the detailed device parameters. We adopt resistance parameters collected by the Michigan State University group for Co/Cu systems [15], *i.e.*, $\varrho_{\text{Co}}^* = 75 \text{ n}\Omega\text{m}$, bulk polarization $\beta = 0.46$, $\varrho_{\text{Cu}}^* = 6 \text{ n}\Omega\text{m}$, $R_{\text{Co/Cu}}^* = 0.51 \text{ f}\Omega\text{m}^{-2}$, and an interface polarization $\gamma = 0.77$. The mixing conductance that agree with first-principles band-structures calculations and ferromagnetic resonance experiments is $R_{\text{Co/Cu}}^* = 1.0 \text{ f}\Omega\text{m}^{-2}$ [8]. The magnetically active region is 10Cu|3Co|10Cu|12Co|35 Cu, where the numbers denote the thickness of the layers in nanometers. The right normal metal thickness is chosen smaller than the geometrical since the nano-pillar widens[12].

Before going into details, we summarize our results for the NYU/IBM samples in Fig. 2 in semi-quantitative agreement with the experiments. Starting in a parallel configuration there is a macrospin instability for ferromagnet 1 at positive currents. The macrospin excitation leads to an antiparallel configuration for larger currents [4], which should be confirmed by spatially dependent micromagnetic calculations. A further increase in the current leads to a spin-wave instability in ferromagnet 2. Similarly, for negative current, we predict a spin-wave instability for ferromagnet 2 [17].

The theoretical Gilbert damping constant is plotted in Fig. 3 for a bulk Gilbert damping $\alpha_{\text{Co}}^{(0)} = 0.003$ for both ferromagnets. Spin-pumping is important, giving rise to a strongly enhanced Gilbert damping constant of the thin ferromagnet that increases with wave vector. Both spin-pumping and spin torque increase with the interface to volume ratio. Ferromagnet 1 is easier to excite but its enhanced damping partially compensates this effect, thus allowing excitations of both ferromagnets to compete. Numerical results for the critical current $\partial j_1 / \partial H$ at high magnetic fields are displayed in Fig. 3 for the thin ferromagnet 1 and the thick ferromagnet 2 for the parallel configuration. For positive

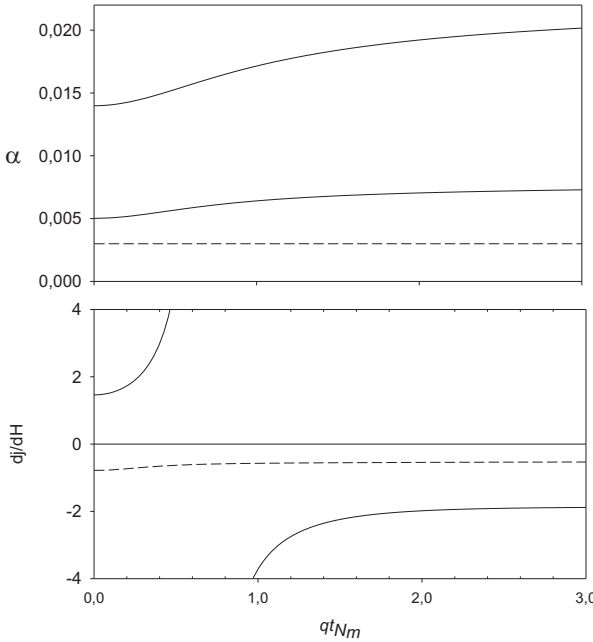


FIG. 3: Upper: Gilbert damping in thin ferromagnet 1 (upper curve), thick ferromagnet 2, and in bulk (dashed line) vs. $qtNm$. Lower: Critical current $\partial j/\partial H$ in units of $10^{12} \text{ Am}^{-2} \text{ T}^{-1}$ of thin ferromagnet 1 (solid line) and thick ferromagnet 2 (dashed line) vs. $qtNm$.

currents, experiments find switching of the thin ferromagnet presumably to an antiparallel configuration when $\partial j^{(c)}/\partial H = 0.6 \times 10^{12} \text{ Am}^{-2} \text{ T}^{-1}$ [12]. This value is extracted from the line in their contour plot of d^2V/dI^2 showing the onset of magnetic excitations. Indeed, for positive currents macrospin excitations occurs first with lowest critical current that agrees well with experiments. Furthermore, we expect spin-wave excitations for the thick ferromagnet 2 at opposite currents, again in good agreement with experiments [12]. Additionally (but not shown here) we predict that after the thin ferromagnet 1 switches, ferromagnet 2 also becomes unstable against spin-wave excitations for positive currents, supported by experiments as well. Residual quantitative discrepancies between experiments and theory are believed to be caused by uncertainties in the material and devices parameter and details in the micromagnetic structure.

In conclusion, we report a theory of macrospin *vs.* spin-wave excitations in spin valves that explains recent observations using only independently determined material and device parameters. The rich phase space of magnetic excitations is classified in terms of macrospin and finite wavelength spin-wave excitations that depend on the resistance distribution in the magnetically active region. For symmetric junctions, macrospin instabilities are strongly favored. Finite wavelength spin-wave excitations are pronounced in asymmetric spin-valves with

relatively high normal metal resistances comparable to that of the ferromagnets. Since the results are in agreement with recent experiments, we are confident that our insights should be helpful to explore the magnetization dynamics in the full parameter space spanned by currents, external magnetic fields, and device design.

A. B. thanks A. D. Kent, B. Özyilmaz, M. Stiles and J. Z. Sun for stimulating discussions. This work has been supported in part by the Research Council of Norway, NANOMAT Grants. No 158518/143 and 158547/431, the Harvard Society of Fellows, the FOM, and EU via NMP2-CT-2003-505587 'SFINX'.

- [1] L. Berger, Phys. Rev. B **54**, 9353 (1996).
- [2] J. Slonczewski, J. Magn. Magn. Mater. **159**, L1, (1996).
- [3] M. Tsoi *et al.*, Phys. Rev. Lett. **80**, 4281 (1998); J.-E. Wegrowe *et al.*, Europhys. Lett. **45**, 626 (1999); E.B. Myers *et al.*, Science **285**, 867(1999); J.A. Katine *et al.*, Phys. Rev. Lett. **84**, 3149 (2000); J. Grollier *et al.*, Appl. Phys. Lett. **78**, 3663 (2001); S. Urazhdin *et al.* Phys. Rev. Lett. **91**, 146803 (2003); S. I. Kiselev *et al.* Nature (London) **425**, 380 (2003); I. N. Krivotorov *et al.* Science **307**, 228 (2005).
- [4] B. Özyilmaz *et al.* Phys. Rev. Lett. **91**, 067203 (2003).
- [5] A. Brataas, Yu.V. Nazarov, and G.E.W. Bauer, Phys. Rev. Lett. **84**, 2481 (2000); Eur. Phys. J. B **22**, 99 (2001); K. Xia *et al.*, Phys. Rev. B 65, 220401 (R) (2002); G. E. W. Bauer *et al.*, Phys. Rev. B **67**, 094421 (2003); M. Zwierzycki *et al.*, cond-mat/0402088.
- [6] X. Waintal *et al.*, Phys. Rev. B **62**, 12317 (2000); M. D. Stiles and A. Zangwill, Phys. Rev. B **66**, 014407 (2002).
- [7] W. Wernsdorfer *et al.* Phys. Rev. Lett. **78**, 1791 (1997); R. H. Koch *et al.* Phys. Rev. Lett. **84**, 5419 (2000).
- [8] Y. Tserkovnyak, A. Brataas, and G. E. W. Bauer, Phys. Rev. Lett. **88**, 117601 (2002); Phys. Rev. B **67**, 140404(R) (2003); for a review, see cond-mat/040924.
- [9] D. M. Apalkov and P. B. Visscher, cond-mat/0405305; T. Valet, unpublished; G. Bertotti *et al.*, Phys. Rev. Lett. **94**, 127206 (2005).
- [10] M. L. Polianski and P. W. Brouwer, Phys. Rev. Lett. **92**, 026602 (2004).
- [11] M. D. Stiles, J. Xiao, and A. Zangwill, Phys. Rev. B **69**, 054408 (2004); T.Y. Chen *et al.* Phys. Rev. Lett **93**, 026601 (2004); B. Özyilmaz *et al.*, Phys. Rev. Lett **93** 176604 (2004).
- [12] B. Özyilmaz *et al.* Phys. Rev. B **71**, 140403(R) (2005).
- [13] K.J. Lee *et al.*, Nature Materials **3**, 877(2004); Z. Li and S. Zhang, Phys. Rev. B **68**, 024404 (2003).
- [14] J. Manschot, A. Brataas, and G. E. W. Bauer, Appl. Phys. Lett. **85**, 3250 (2004).
- [15] J. Bass and W. P. Pratt Jr., J. Magn. Magn. Mater. **200**, 274 (1999).
- [16] J. Z. Sun *et al.*, proceedings of the 49th MMM 2004.
- [17] After submitting our article, the Cornell collaboration, S. I. Kiselev *et al.*, cond-mat/0504402, publish high-frequency measurements that provide direct evidence that the interpretation in Ref. [12] and the present calculations are correct.